THE JOURNAL OF PHYSICAL CHEMISTRY Letters

PERSPECTIVE

pubs.acs.org/JPCL

Photoelectron Transfer in Zeolite Cages and Its Relevance to Solar Energy Conversion

Prabir K. Dutta* and Michael Severance

Department of Chemistry, The Ohio State University, 100 West 18th Avenue, Columbus, Ohio 43210, United States

ABSTRACT: The cages and channels of aluminosilicate zeolites provide a novel environment for molecular and nanoparticle assembly for photochemical reactions. In their dehydrated forms, zeolites can be active participants in reactions with photoexcited entrapped molecules as electron donors and acceptors. The charge-separated species thus formed are stabilized for hours. With hydrated zeolites, the encapsulation and the restricted mobility can result in long-lived charge-separated species. In order to exploit intrazeolitic photoelectron transfer, the role of structural defects, steric effects, electrostatic polarizing fields, and extraframework cations in formation and stabilization of charge-separated species needs to be better elucidated. Such efforts will be facilitated with better control of synthesis of molecular and nanoparticle assemblies within the zeolite, rather than the random distribution mostly practiced to date. Artificial photosynthetic assemblies within zeolites aimed toward practical photolytic water splitting have potential because of varied ways of charge transport, including via the framework or molecules, as well as the synthesis of zeolite membranes that can propagate light, cations, and electrons over macroscopic distances. Assembly of catalysts capable of multielectron/hole processes within and at zeolite interfaces needs to be coupled with photochemical systems. Better integration strategies for combining efficient light collection, directed charge separation/propagation, and catalysis are necessary for practical impact.

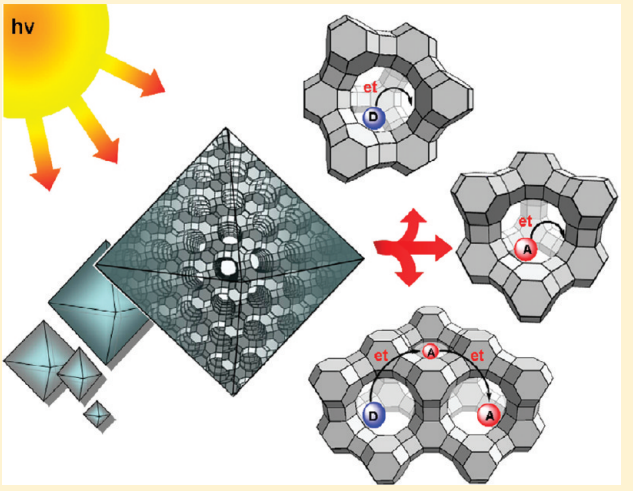

Solar-energy-driven chemistry is a potentially new way of generating fuels and chemicals without the environmental and geopolitical hazards currently facing society. However, these chemistries, which in many cases involve redox reactions, for example, formation of H_2 from water, are complex, and suitable architectures will be necessary.[1−3] Nature provides suitable models of such architecture, and biomimetic approaches are being actively researched. Photosynthesis, which makes possible life on earth, involves collection, conversion, and storage of solar energy as chemical energy. Mediated by an enzyme, photosystem II uses light energy to make oxygen, protons, and electrons from water.[4] The electrons are used by photosystem I along with light to reduce nicotinamide adenine dinucleotide phosphate, whereas the protons generate a transmembrane electrochemical potential that drives ATP synthesis. The architecture necessary to accomplish this is a sophisticated assembly of pigments, enzymes, and proteins in a membrane scaffold. For a practical artificial photosynthesis system, the efficiencies of the solar to chemicals process have to exceed 10%. The successful assembly of superstructures necessary to accomplish these goals requires both fundamental and technological breakthroughs.

Microheterogeneous systems such as vesicles,[5] clays,[6] mesoporous materials,[7] and zeolites[8] are being actively studied as host systems for assembly of photoactive units. In this Perspective, we focus on zeolites, with primary emphasis on light-driven electron transfer and photocatalysis for H_2 formation from water, the fundamental ingredients for solar energy conversion.

Brief Primer on Zeolites. Zeolites are microporous, crystalline aluminosilicates with the framework made up of T—O—T (T = Si, Al) bonds and enclosed cages and channels of molecular dimensions.[9] Figure 1a−d shows the topology of several zeolites, including zeolites L, Y, ZSM-5, and the titanosilicate ETS-4, respectively (along with a 3-D perspective); these frameworks have been the most examined for studies relevant to this Perspective.

Zeolite synthesis typically takes place in an aqueous medium, and over 140 frameworks are known.[10] Because the aluminosilicate framework carries a negative charge, extraframework cations are present as charge-balancing units within the porous framework. Neutral molecules are typically introduced into the empty zeolite after removal of intrazeolitic water, whereas charged cations can be introduced via ion exchange in aqueous

Received: November 4, 2010
Accepted: February 4, 2011
Published: February 14, 2011

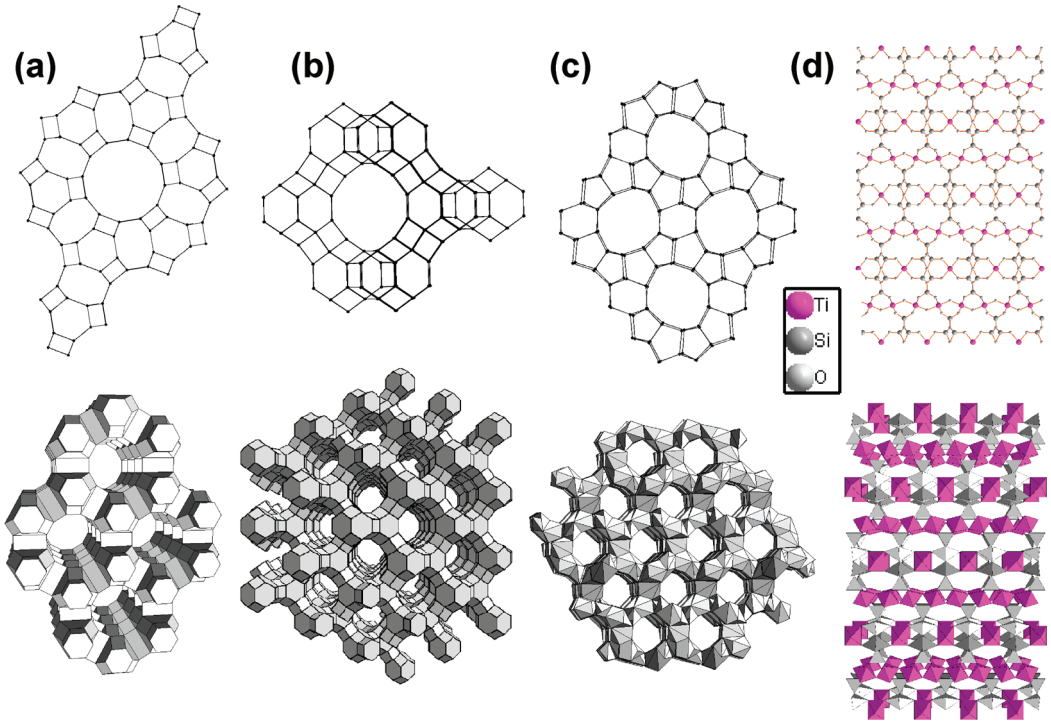

Figure 1. Stick and three-dimensional models of zeolites (a) L, (b) Y, (c) ZSM-5, and (d) titanosilcate ETS-4.

media. The three-dimensional architecture of zeolite imposes a spatial distribution of the internalized molecules, modified by the location and size of the extraframework cations. The Si/Al ratio of the framework can be altered, thereby changing the hydrophilicity of the zeolite. Dehydration of zeolite leads to cation rearrangement, framework distortions, and polarizing electric fields for aluminum-containing zeolites. The Si and Al can be replaced with other atoms, including transition-metal ions, giving rise to redox-active frameworks.

Zeolites have large optical band gaps and behave as insulators. Though they exhibit no electronic conductivity, impedance spectroscopy indicates that ionic conduction via the cations undergoing intracage as well as longer-range intercage motions is possible.[11] Various zeolite morphologies are readily available, ranging from nanometer-sized particles to macroscopic membranes. The structure of zeolites is typically identified from their X-ray powder diffraction patterns. These patterns do not typically provide information on the nature of crystalline or molecular defects. Such defects would include dislocations, twinning, intergrowths of different phases, and stacking faults.[12] Implications for such defects are that the arrangement of encapsulated molecules would be discontinuous as well as restricted access to certain parts of the crystal.[13] Crystalline defects are observed by high-resolution transmission electron microscopy (HRTEM) and atomic force microscopy. There are also framework defects that intercept the local order. These have been categorized as framework or structural defects (e.g., vacancy, peroxy bridges), impurities (e.g., anion and cation substitutions on the framework), and coordination defects involving altered coordination (under- or overcoordination) of the framework atoms.[14] Among electronic defects are self-trapped localized/delocalized holes arising from electron loss or paramagnetic centers from electron gain. These defects are much harder to identify and can change drastically depending on sample preparation and treatment, including ion exchange, dehydration, and in the presence of certain reactive extraframework cations, such as protons. The role of molecular defects on light-activated processes discussed in this Perspective can be profound and not easily recognized or quantified.

Novel effects involving the participation of the zeolite framework and the extraframework cations upon photoexcitation of encapsulated molecules are mostly realized in dehydrated zeolites.

Long-Lived Light-Driven Charge Separated Species: Involvement of the Zeolite Framework. Novel effects involving the participation of the zeolite framework and the extraframework cations upon photoexcitation of encapsulated molecules are mostly realized in dehydrated zeolites. A representative example is diphenylacetylene (DPA) in the zeolite ZSM-5.[15] DPA at a loading level of ~1 molecule/unit cell penetrated through the channels over a period of several months at 300 K. On the basis of the electronic spectrum, it was concluded that encapsulation did not alter the ground state, though Raman spectroscopy did indicate small frequency shifts for Li^+ and Na^+ exchanged zeolites, whereas with bulkier cations (K^+, Rb^+, Cs^+), new bands in the ring-breathing and ring-stretching regions with weak intensity were observed. This suggests that at some small fraction of sites, the molecular geometry is altered (ideal D_{2h} symmetry). Monte Carlo simulations indicated that the DPA molecules are located

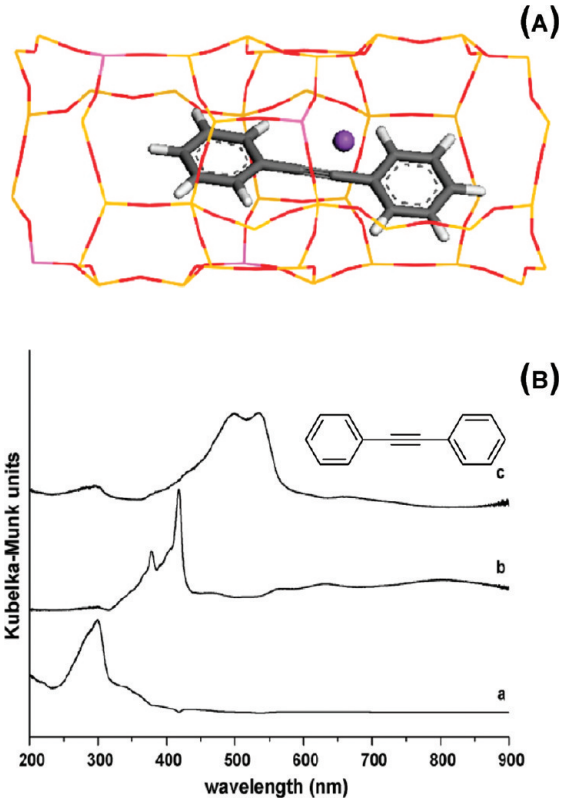

Figure 2. (A) The predicted sorption sites for DPA in the straight channels of NaZSM-5. The purple sphere represents the Na^+ cation. (B) Resolved spectrum of species using multivariate curve resolution of data obtained upon photolysis of (a) unreacted DPA-LiZSM-5, (b) $DPA^{\bullet+}$-LiZSM-5, and (c) DPA-LiZSM-$5^{\bullet-\bullet+}$ (taken from ref 15 with permission).

at the intersection of the straight channel (0.53 × 0.56 nm) with the sinusoidal channel (0.51 × 0.55 nm). The Li^+ and Na^+ interact with the triple bond, whereas K^+, Rb^+, and Cs^+ are facially coordinated to the phenyl group. Figure 2A shows the geometry of DPA in NaZSM-5.

Upon cw photoexcitation into the ~300 nm band (266 nm excitation, 15 s), photoelectron transfer from DPA occurred, with resultant dynamics that lasted for days and was dependent on the extraframework cations. Figure 2B shows the three spectral components that were obtained by multivariate curve resolution of the spectrum obtained upon photoexcitation of DPA in LiZSM-5. Figure 2B(a) is indicative of the unreacted DPA-LiZSM-5. The species with bands at 378, 417, and 795 nm shown in Figure 2B(b) are characteristic of the $DPA^{\bullet+}$ radical cation. In addition, there is a third species with a broad band between 400 and 500 nm and bands at 495 and 535 nm shown in Figure 2B(c). The spectral signature of this third species has also been observed upon photoionization of biphenyl,[16] naphthalene,[17] *t*-stilbene,[18] and *p*-terphenyl[19] in zeolites and assigned to a species formed by electron donation from the zeolite framework to $DPA^{\bullet+}$ and depicted as DPA-ZSM-$5^{\bullet-\bullet+}$. The electronic band in Figure 2B(c) has been assigned to a charge transfer from DPA to zeolite in the species DPA-ZSM-$5^{\bullet-\bullet+}$. The cations have a profound influence on the dynamics of the two charge-separated species, $DPA^{\bullet+}$ and DPA-ZSM-$5^{\bullet-\bullet+}$. Only in the case of LiZSM-5, are both $DPA^{\bullet+}$ and the DPA-ZSM-$5^{\bullet-\bullet+}$ observed, whereas DPA-ZSM-$5^{\bullet-\bullet+}$ is only observed for Na, K, Rb, and Cs ZSM-5. Both species $DPA^{\bullet+}$ and the DPA-ZSM-$5^{\bullet-\bullet+}$ decay with time, and electronic and Raman spectroscopy indicate that the initial DPA-ZSM-5 is eventually recovered. For LiZSM-5, the decay rate constants for $DPA^{\bullet+}$and DPA- ZSM-$5^{\bullet-\bullet+}$ are ~0.055 and ~0.0078 min^{-1}, respectively. The decay of the electron−hole pair in DPA-ZSM-$5^{\bullet-\bullet+}$ to the initial state follows the order $Cs^+ > Rb^+ \approx K^+ > Na^+ > Li^+$ and correlates with increasing basicity of the framework with increasing cation size. The initial electron acceptor from photoexcited DPA to form the radical cation is unknown; a possibility is the Na_4^{3+} cluster, though it was not identified spectroscopically in the DPA-ZSM-5 sample.

In the case of *p*-terphenyl in ZSM-5, EPR measurements showed that the electron and hole in ZSM-$5^{\bullet-\bullet+}$ intermediate species are located on the oxygen atoms of the Si—O—Al close to the extraframework cation (Li^+).[19] The formation of the electron−hole pair (ZSM-$5^{\bullet-\bullet+}$) has been noted for *p*-terphenyl, biphenyl, *t*-stilbene, and naphthalene with $E_o$values (vs SCE) of 1.78, 1.9, 1.75, and 1.54 V, respectively for the corresponding radical cation. Similar electron abstraction from the framework was not observed for the anthracene radical cation (1.1 V), indicating a threshold for the electron-donating species on the zeolite.[20]

The reasons for the long-lived charge separation (hours) in these systems is not well understood, and confinement of the organic molecules, electron−hole migration, as well as strong polarizing fields from the cation−framework interactions are implied as responsible for the long-lived charge separation. No photoionization was observed in the completely siliceous form of ZSM-5, silicalite for the DPA system. Without ultrafast spectroscopy, it is unclear if the photoionization phenomena do not occur or if the back electron transfer dynamics is rapid.

Another novel role of the zeolite framework is its ability to transfer photochemically generated electrons and holes from donor to acceptor molecules through empty cages.[21,22] Such effects have been demonstrated in zeolite NaY using *trans*-anethole as the electron donor (photoexcitation 308 nm) and

The reasons for the long-lived charge separation (hours) in these systems is not well understood, and confinement of the organic molecules, electron−hole migration, as well as strong polarizing fields from the cation−framework interactions are implied as responsible for the long-lived charge separation.

1,4-dicyanobenzene as the electron acceptor. Electron migration took place over ~11 Å (approximately a supercage). The electron injection into the zeolite upon photoexcitation of *trans*-anethole is very fast ($\geq 10^8$ s^{-1}), with spectroscopic evidence that the electron is accommodated on Na_4^{3+} clusters (a transient band at 400−700 nm). However, the Na_4^{3+} clusters disappeared rapidly (μs), whereas the anethole radical cation was

dx.doi.org/10.1021/jz101500z |*J. Phys. Chem. Lett.* 2011, 2, 467–476

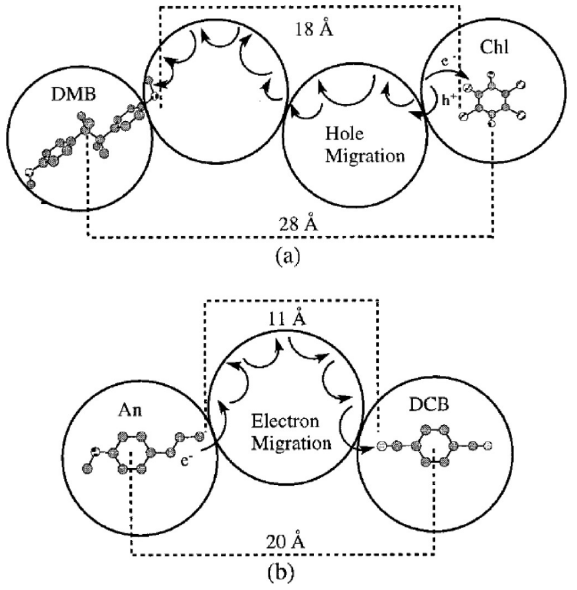

Figure 3. Schematic of proposed (a) hole migration from photoexcited chloranil (Chl) to 4,4′-dimethoxybicumene (DMB) and (b) electron migration from photoexcited anethole (An) to 1,4-dicyanobenzene (DCB). (Taken from ref 21.)

stable (decay rate constant of 3.3×10^4 s^{-1}). For high loading levels of 1,4-dicyanobenzene (DCB, 1 molecule per supercage), direct electron transfer from photoexcited anethole to dicyanobenzene occurred, but the back electron transfer was also very rapid in this geminate arrangement. With lower loadings of dicyanobenzene, both the anethole radical cation (380, 600 nm) and the dicyanobenzene radical anion (340, 430 nm) are formed and are long-lived with comparable decay rate constants of $\sim 10^3$ and 10^4 s^{-1} for both species. These studies concluded that the zeolite is actively involved in the charge-transfer process, first as an electron acceptor from anethole and second as serving to move this electron across intrazeolitic space to the DCB. Optimal charge separation was noted for Na^+-exchanged zeolite Y. With the larger cations (K^+, Rb^+, Cs^+), only direct electron transfer between anethole and DCB was noted; the zeolite framework became increasingly basic with larger cations and therefore not as good of an electron acceptor from photoexcited anethole, leading to the shorter lifetimes of the anethole radical cation. Hydration of the zeolite completely impedes long-range electron transfer.

Photoexciting chloranil in Na-zeolite Y led to abstraction of an electron from the zeolite and hole migration via the framework to 4,4′-dimethoxybicumene over through-space distances of 18 Å. Photoexcitation of chloranil leads to the formation of the triplet state and is the likely reactant with the framework (singlet reactivity is possible, but less likely because of rapid intersystem crossing). Transient diffuse reflectance studies show that a fraction of the triplet species participates in the electron transfer, indicating heterogeneity in zeolite donor sites.

Figure 3 shows the proposed models for electron and hole migration. The exact mechanism of electron transport is not known, and the role of electron-deficient sites such as cations, cation clusters, and aluminum centers was considered. Also, the migration along the framework possibly involves much longer distances than the average 11 Å calculated for through-space transfer. The dominant electron-donation sites for creation of holes in the chloranil system were proposed to be lattice oxygens (Si—O—Al) and also as conduits for hole transfer. Excitation within the band gap of microporous germanosilicates at 266 nm leads to electron−hole separation, and in the presence of encapsulated molecules, radical cations or anions are formed with long lifetimes.[23] Evidence for migration of the holes/electrons along the framework as with zeolites was also noted in the germanosilicates.[23]

Electron donation from zeolite to methylviologen[24] and 1,2,4,5-tetracyanobenezene[25] resulting in long-lived charge-separated species has also been reported. Both the role of the polarizing electrostatic fields and the possibility that the framework can promote charge migration have been considered for explaining the long-lived charge transfer.

There are several consistent themes that emerge from these light-driven charge-transfer processes in dehydrated zeolites.

- The zeolite framework/extraframework cations can be involved in electron−hole transfer to photoexcited molecules encapsulated in its pores.
- The zeolite backbone and cations can facilitate electron−hole transfer over nanometer distances.
- The charge-separated species are created very fast but can survive on the time scale of hours/days.
- Electron−hole transfer between molecules can be mediated through the zeolite framework.
- Extraframework cations and framework composition (Si/Al ratio) influence the charge separation process.
- Intrazeolitic water and completely siliceous forms of the zeolite completely inhibit the long-lived charge separation phenomena.

Photochemical Charge Transfer in Hydrated Zeolites. Several studies have focused on intermolecular light-driven photoelectron-transfer reactions in hydrated zeolites. In these cases, the role of the framework is to constrain the molecules, as well as position them in three-dimensional arrangements consistent with the zeolite topology.

Many of these studies have focused on polypyridyl complexes of ruthenium, in particular, $Ru(bpy)_3^{2+}$, which because of its ∼12−13 Å size can be securely trapped within the supercage of the faujasitic framework (∼13 Å). Deuterium NMR studies of $Ru(bpy)_3^{2+}$ with deuterated bpy ligands encapsulated in the zeolite have shown that the molecule has no rotational motion at room temperature and only slight motion at 373 K.[26] However, the spectroscopic features, including absorption, emission spectra, and lifetimes are comparable to solution as long as the loading is kept low so that the population of neighboring cages with $Ru(bpy)_3^{2+}$ is insignificant.[27]

Electron transfer from photoexcited encapsulated $Ru(bpy)_3^{2+}$ to bipyridinium ions with varying reduction potentials in neighboring zeolite Y cages has been extensively studied.[28] The major conclusion was that the back electron transfer from the bipyridinium radical cation to $Ru(bpy)_3^{3+}$ is slowed down by several orders of magnitude ($\sim 10^4$ s^{-1}) as compared to that in solution. Immobilization of the $Ru(bpy)_3^{2+}$ in the supercage was proposed as the primary reason for slowing of the back electron transfer to Ru^{3+}, though forward electron transfer via the $bpy^{\bullet -}$ localized on the photoexcited ligand-to-metal charge-transfer state to the viologen-like ions in the neighboring supercage can readily occur (>10^7 s^{-1}).

This concept of inflexibility of the ruthenium unit was extended by use of a ligand L_{DQ} (1-[4-(4′-methyl)-2,2′-bipyridyl]-2-[4-(4-*N*,*N*′-tetramethylene)-2,2′-bipyridyl]ethane);

dx.doi.org/10.1021/jz101500z |*J. Phys. Chem. Lett.* 2011, 2, 467–476

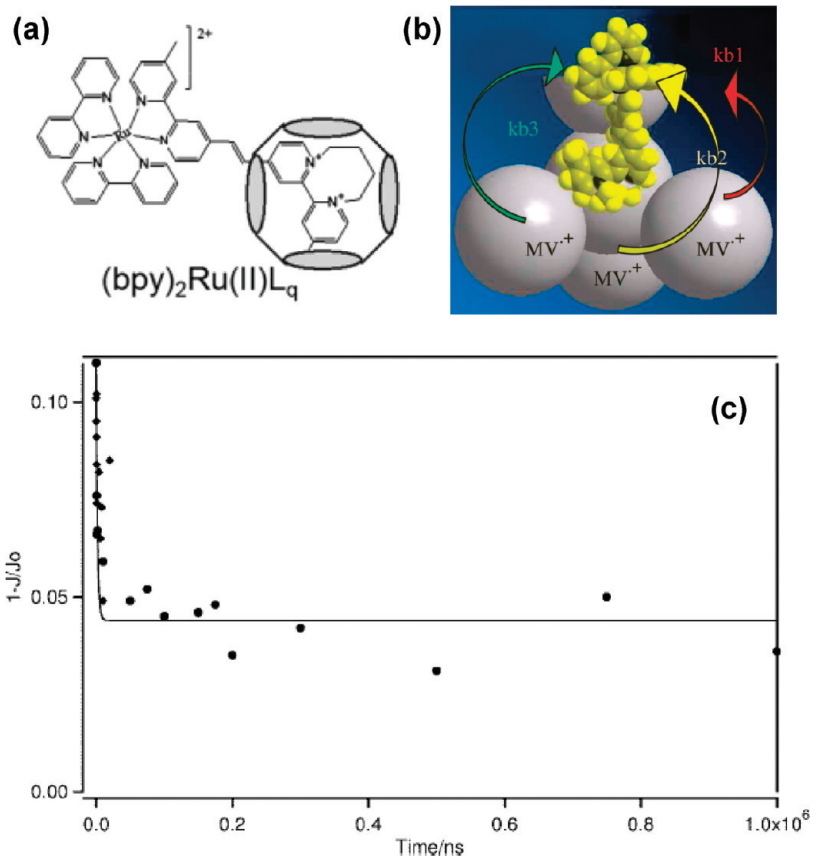

Figure 4. (a,b) Schematic of $(bpy)_2RuL_{DQ}$ held on the zeolite surface. (c) Plot of the intensity of the 390 nm band of the methylviologen radical obtained from the transient diffuse reflectance spectrum of $(bpy)_2RuL_{DQ}/MV^{2+}$/zeolite (as shown schematically in b). (Taken from ref 29.)

the $(bpy)_2RuL_{DQ}$ ligand was attached to the surface of zeolite crystals, and the electron-transfer dynamics to bipyridinium ions within the zeolite was monitored.[29] Figure 4a shows that the inflexibility in L_{DQ} arises from the double bond, and Figure 4b shows a schematic of the $(bpy)_2RuL_{DQ}$ held in a zeolite cage surrounded by methylviologen (MV^{2+}) in neighboring cages. Upon photoexcitation, the characteristic band due to the methylviologen radical cation (390 nm) in the zeolite is observed, and the time dependence of the decay of the 390 nm band is shown in Figure 4c. About 40% of the radical cation is stabilized on the millisecond time scale. The back electron transfer rate of 3×10^5 s^{-1} from the methylviologen radical cation to Ru(III) (k_b in Figure 4b) is significantly slower as compared to the forward electron transfer (10^7 s^{-1}) .

Electron transfer between $Ru(bpy)_3^{2+}$ and other electron acceptors in hydrated zeolite has also been examined. These include the 2,4,6-triphenylpyrilum ion, which is also synthesized within the zeolite by a ship-in-a-bottle approach.[30] Much like the $Ru(bpy)_3^{2+}$-bipyridinium studies, transient spectroscopy indicates the formation of $Ru(bpy)_3^{3+}$, and its lifetime is longer than hundreds of microseconds, indicating that back electron transfer from the neutral triphenylpyrilum to $Ru(bpy)_3^{3+}$ is slowed down in the zeolite. It is also important to note that $Ru(bpy)_3^{3+}$ is completely formed within the laser pulse duration (10 ns), indicating rapid forward electron transfer.

The theme that emerges from these studies is that in hydrated zeolites, the dynamics of electron transfer is influenced strongly by encapsulation since the rigidity of the framework inhibits motion of the molecules. The slow back electron transfer within zeolites has been exploited to create charge-separated species on a permanent time scale by steady-state photolysis. One of the first studies was to use the zeolite-encapsulated $Ru(bpy)_3^{2+}$-bipyridinium system (DQ^{2+}, *N*,*N*′-tetramethylene-2,2′-bipyridinium) with propylviologen sulfonate (PVS is a zwitterionic neutral molecule) in solution surrounding the zeolite.[31] Upon visible light illumination, $PVS^{\bullet-}$ was formed in the solution. The proposed model involved electron transfer from photoexcited $Ru(bpy)_3^{2+*}$ to bipyridinium ion DQ^{2+} within the zeolite and electron hopping across the DQ^{2+} to the zeolite−water interface, where vectorial electron transfer (driving force ≈ 240 mV) to PVS took place. The quantum yield (457 nm) of charge separation was estimated to be 0.05%.

The theme that emerges from these studies is that in hydrated zeolites, the dynamics of electron transfer is influenced strongly by encapsulation since the rigidity of the framework inhibits motion of the molecules.

dx.doi.org/10.1021/jz101500z |*J. Phys. Chem. Lett.* 2011, 2, 467–476

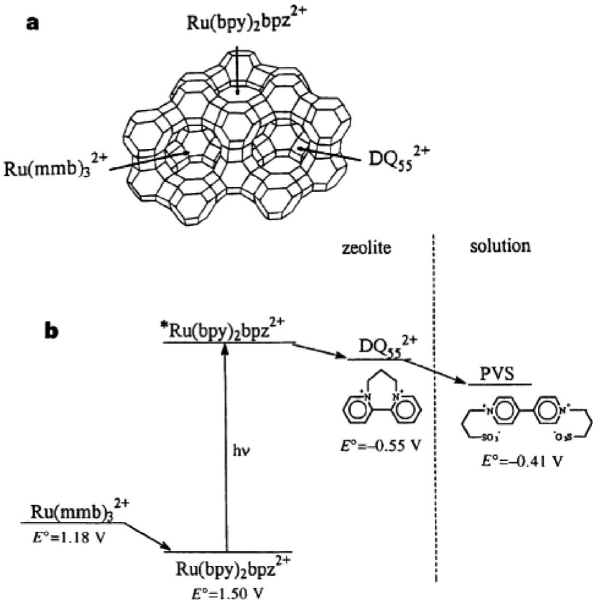

Figure 5. (a) Schematic representation of the assembly of donor Ru(mmb)$_3^{2+}$ and sensitizer Ru(bpy)$_2$(bpz)$^{2+}$ in neighboring cages and then the zeolite ion-exchanged with DQ^{2+}. (b) Electron-transfer process taking place in the zeolite and at the zeolite−solution interface; the neighboring donor−acceptor assembly by design leads to improved charge transfer. (Taken from ref 33 with permission.)

The (bpy)$_2$RuL$_{DQ}$ was also incorporated on the surface of a zeolite membrane, with the zeolite cages being occupied by *N*,*N*′-trimethyl-2,2′-bipyridinium ion. Visible light illumination of the Ru complex side of the membrane in the presence of a sacrificial electron donor led to formation of PVS$^{\bullet-}$ on the other side of the membrane, indicating charge propagation through the membrane over macroscopic distances.[32]

A novel adaptation of this strategy was accomplished by incorporating two complexes, Ru(bpy)$_2$(bpz)$^{2+}$ and Ru(mmb)$_3^{2+}$, in neighboring supercages of zeolite Y by design (mmb in 5-monomethyl-2,2′-bipyridine, bpz in 2,2′-bipyrazine), as shown in Figure 5.[33] This is the only known example where two molecules in neighboring cages are uniformly made in the zeolite; in most cases, the incorporation method ensures that the molecular distribution is random. Upon photoexcitation of Ru(bpy)$_2$(bpz)$^{2+}$ (473 nm), electron transfer to DQ^{2+} takes place. The presence of neighboring Ru(mmb)$_3^{2+}$ sets up a competition between back electron transfer from the DQ$^{\bullet+}$ radical to Ru(bpy)$_3^{3+}$ and Ru(mmb)$_3^{2+}$ to Ru(bpy)$_3^{3+}$. The presence of Ru(mmb)$_3^{2+}$ results in a 4-fold increase in the efficiency of PVS$^{\bullet-}$ generation in solution.

As charge transfer from the zeolite to PVS occurs across the zeolite−solution interface, a cation also has to be released into solution to maintain charge neutrality. By using a K$^+$-entrapping crown ether in solution (the solvent was acetonitrile), the yield of the bipyridinium ion radical in solution was increased by a factor of ∼10 upon illumination of a K$^+$-exchanged Ru(bpy)$_3^{2+}$-encapsulated zeolite Y.[34] Thus, the complexation of the migrating ion is another way to improve steady-state charge separation yields.

In these steady-state experiments, the photogenerated electron appears on the bipyridinium ion in solution, suggesting that a Ru^{3+} state must be present in the zeolite. However, attempts at obtaining spectroscopic evidence for the Ru^{3+} state have been

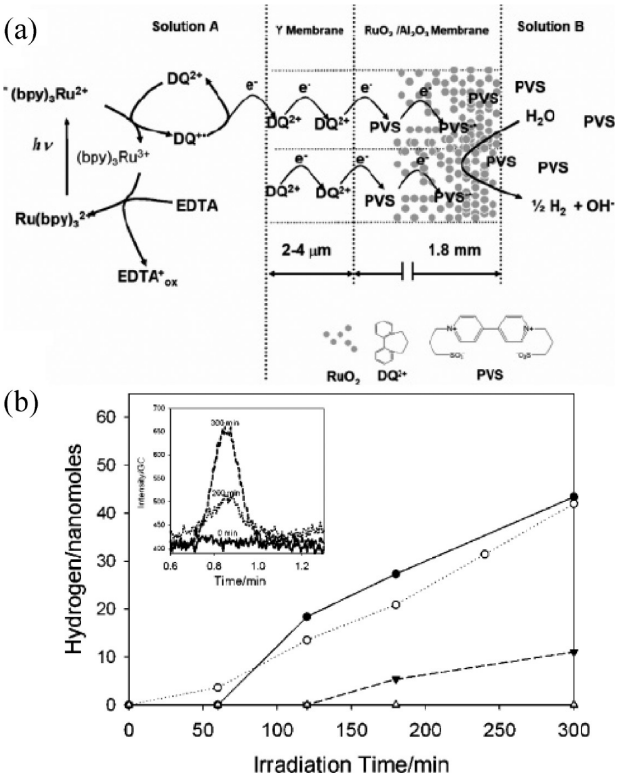

Figure 6. (a) Schematic of the zeolite Y membrane-based H$_2$ evolution system. Solution A on the left of the membrane contains 0.5 mM Ru(bpy)$_3^{2+}$, 40 mM EDTA, and 25 mM DQ^{2+}. Solution B contains 141 mM PVS and is on the right side of the zeolite membrane. The Al$_2$O$_3$ support used for the zeolite membrane contains RuO$_2$ as the catalyst. (b) H$_2$ evolution data with the membrane assembly shown in (a); (•, ○) represent two different zeolite Y membranes extensively ion-exchanged with DQ^{2+} and solutions A and B, as identified in (a). These data show the reproducibility of different membrane preparations. The inset shows typical GC traces used measuring H$_2$. (Δ) represents a control experiment without any DQ^{2+} in solution A or in the zeolite membrane. (▼) represents a similar experiment as that in (○, •) but with the zeolite membrane without any DQ^{2+}. The delay in the onset of H$_2$ evolution corresponds to the time taken for DQ^{2+} to exchange into the zeolite. (Taken from ref 36).

unsuccessful; only the Ru^{2+} is observed. Thus, there are suggestions that in the aqueous systems, water may act as the donor, and in nonaqueous systems, this role is played by the zeolite, in both cases reducing Ru^{3+}.

The themes emerging from the steady-state experiments are as follows:

- The zeolite architecture, by virtue of arrangement of molecules, makes it possible to transport charge across macroscopic distances.
- The zeolite−solution interface allows for photogenerated charge within the zeolite to be moved into solution, thus providing opportunities for further chemistry.
- Extraframework cation motions influence charge transport
- Quantum yields of permanent charge separation are low (∼10^{-3}−10^{-4}).

Besides molecular assembles, the microporous space in zeolites has also been used as a host for semiconductors and metals. In the dehydrated state of the zeolite, the framework has a major influence on the optical properties of the nanometer-sized encapsulated solids. Upon hydration, these clusters typically

dx.doi.org/10.1021/jz101500z |*J. Phys. Chem. Lett.* 2011, 2, 467–476

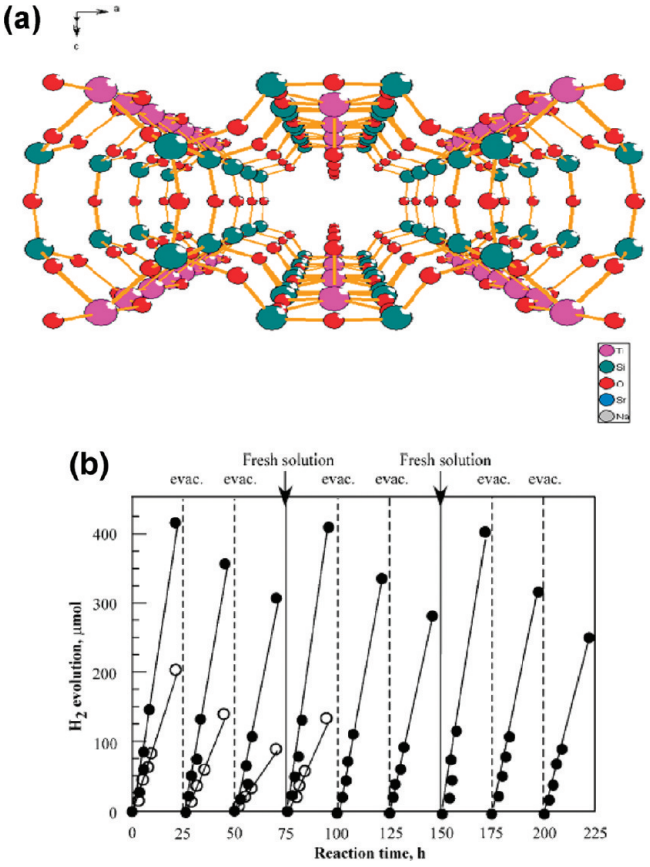

Figure 7. (a) ETS-4 pore openings as well as a view of the Ti—O—Ti nanowire arrangement in ETS-4. (b) Comparison of H_2 evolution over the CdS/ETS-4 (•) and bulk CdS (0) under visible light irradiation (catalyst 0.1 g in 60 mL of 0.1 M Na_2S, 0.5 M Na_2SO_3, and 1.0 M NaOH solution). (Taken from ref 41 with permission.)

are forced out of the zeolite framework, especially in hydrophilic aluminum-containing zeolites. However, the hydrated semiconductor zeolites are finding applications in artificial photosynthesis assemblies and are therefore of practical relevance.

Zeolite-Based Artificial Photosynthetic Systems: Water to H_2 Formation. We primarily focus on artificial photosynthetic models based on zeolites involving the light-driven splitting of water to hydrogen. Both molecular assemblies and semiconductor-based systems have been investigated.

Molecular-Based Assemblies. The formation of hydrogen from water necessitates the use of a catalyst. The internal architecture of the zeolite makes this possible. One of the first reports of a zeolite-based assembly for evolution of H_2 from water was a $Ru(bpy)_3^{2+}/MV^{2+}/Pt$ assembly in mordenite.[35] The mechanism proposed involved electron transfer from $Ru(bpy)_3^{2+*}$ to TiO_2, with MV^{2+} mediating electron transfer from the TiO_2 to Pt; sacrificial electron donors (TEOA, EDTA) were used, and the quantum yield for H_2 evolution was ~1% (450 ± 5 nm excitation). Hydrogen evolution was also observed with $Ru(bpy)_3^{2+}/Nb_2O_5/Pt$, and quantum yields of 1% were observed with sacrificial donors, and about 0.01% was observed with nonsacrificial donors.

The $Ru(bpy)_3^{2+}$-based sensitizer and bipyridinium system (DQ^{2+}) discussed earlier was incorporated into a zeolite membrane, as shown in Figure 6a. Insertion of a RuO_2 catalyst into this architecture led to a photochemical water to H_2 conversion, as shown in Figure 6b.[36] Several unique properties of the zeolites as well as the membrane/support architecture were exploited. These include the charge propagation through the zeolite membrane by electron hopping via the bipyridinium ions that occupy the supercages. The porous alumina that acts as the support for the zeolite film was also used as the support for the RuO_2 catalyst as well as the PVS necessary for hydrogen formation. The yields of this process were comparable to that for a mixture of $Ru(bpy)_3^{2+}$ bipyridinium ions and catalyst, indicating that the zeolite membrane is serving to spatially separate the electron and hole. The relevance of this study demonstrates that photogenerated electrons can traverse through the zeolite membrane, be spatially separated, and be used for the reduction of water.

Evidence for charge hopping via zeolite-encapsulated bipyridinium ions was demonstrated in an earlier chemical experiment.[37] Addition of a sodium salt of carbonylmanganate donors ($Mn(CO)_4L^-$, L = CO, $P(OPh)_3$, an anion that cannot penetrate into the zeolite) to a methylviologen-loaded zeolite Y quantitatively reduced all of the intrazeolitic methylviologen to the cation radical. This is only possible if the initial reduced methylviologen near the surface of the zeolite particle can transmit electrons into the interior of the zeolite and needs to occur by a self-exchange process.

Semiconductor Assemblies. The other type of architecture that has resulted in light-driven activation of molecules to produce hydrogen is semiconductor—zeolite composites, in particular, CdS. For synthesis of CdS in zeolites, the common procedures are ion exchange of Cd^{2+} in the zeolite, followed by reaction with H_2S or Na_2S. For the H_2S-based procedure, the experiments can be carried out with dehydrated zeolites. Several studies have reported the synthesis of CdS in zeolites and examined H_2 generation with visible light.[38] The exact location of the CdS and its mobility have only been recently confirmed. Careful experiments have shown that intrazeolitic CdS clusters can be assembled only under strict anhydrous conditions.[39] Humidity forces the CdS clusters out of the zeolite and also leads to partial zeolite degradation. Recently, synthesis of CdS in hydrophobic zeolites (silicalite) has been reported, and in this case, the intrazeolitic clusters are stable because water is repelled by the zeolite.[40]

Combining CdS and TiO_2 is known to improve the H_2 generation efficiency because the electon—hole recombination is minimized due to electron transfer to TiO_2 from photoexcited CdS. Thus, several strategies have been reported for using zeolite hosts to make the compound semiconductor system. One of these strategies was to use titanosilicate zeolites as the host. The titanosilicates (ETS series) contain chains of corner-linked TiO_6 octahedra and can be considered to be Ti—O—Ti—O nanowires of 0.67 nm diameter and spanning the length of the crystal (Figure 7a). Upon visible light photoexcitation of CdS embedded in/on ETS-4, H_2 evolution was observed in the presence of S^{2-}/SO_3^{2-} as a sacrificial electron donor.[41] Figure 7b shows the comparison of the H_2 evolution between bulk CdS and CdS/ETS-4, demonstrating marked improvement with the ETS sample. Electron transfer from photoexcited CdS to the Ti—O—Ti nanowire was proposed as the key step, followed by water reduction by titania. The quantum yields of the CdS/ETS-4 and CdS/ETS-10 (420 nm) for H_2 production were determined to be 0.42 and 0.31%, respectively. It was also reported that incorporation of CdS into the zeolite slows down its photocorrosion.

dx.doi.org/10.1021/jz101500z |*J. Phys. Chem. Lett.* 2011, 2, 467–476

Critical Analysis. It should be apparent from the discussion above that light-driven electron-transfer reactions of species in zeolites are influenced by several characteristic properties of this host.

- Topological spatial arrangement of molecules controlled by the zeolite structure and their restricted motions.
- In dehydrated zeolites, molecules experience strong electrostatic fields and interact with barely solvated cations and are therefore subject to strong polarization.
- In dehydrated zeolites, the framework can mediate electron and hole transfer over tens of Angstroms.
- Constrained motion of encapsulated molecules slows geminate charge recombination rates in hydrated zeolites.
- Long-range charge motion can occur within zeolites by charge hopping between adjacent encapsulated molecules.
- Semiconductor and other nanoparticles can be assembled within dehydrated zeolite cages. In aluminous hydrophilic zeolites, water will displace the nanoparticles and promote aggregation on the zeolite surface.

The advantage of supramolecular chemistry arises because placement of specific molecules in a particular geometry gives rise to novel behavior. This is best illustrated in photosynthetic systems, where light collection occurs by an antenna complex, with chlorophyll molecules arranged in a particular geometry.[4] Efficient electron transfer occurs in the reaction center by specific arrangement of proteins in a membrane.

Because the zeolite cages/channels have an organized three-dimensional structure, molecules in these cages will follow this topology. The best match between the topology and molecular arrangement is realized with saturation loading. Thus, at a loading of ~1.5 molecules of methylviologen per supercage, the MV^{2+} molecules are arranged in a tetrahedral diamond-like extended lattice. Electron exchange takes place across the zeolite crystal,[31,33] or even a zeolite membrane.[32,36] Dye molecules such as thionine packed in zeolite L one-dimensional channels can transport energy by Forster energy transfer over the entire length of the crystallite.[8]

However, as soon as loading levels are below the saturation limit, then there is a random distribution of the molecules, and their spatial relationship is not uniquely identified by the zeolite topology. Statistical analysis provides probabilistic information on the number of neighboring molecules as a function of distance and has been used for investigating energy/electron transfer of molecules.[21,22,27]

Synthesis strategies for creating species in specific neighboring positions such as A···A, A···B, and A···B···C at controlled loadings will facilitate a more quantitative understanding of the influence of zeolite on photochemical processes. The only published example of a molecular assembly by design is the A···B complex with A and B in neighboring supercages, as shown in Figure 5.[33] All other reported attempts of binary and ternary systems in zeolite are essentially a statistical distribution and thus not optimized. For example, charge separation yields were lower for $Ru(bpy)_3^{2+}$-triphenylpyrilium with TiO_2 in the zeolite, but it is impossible to estimate the true mechanism without knowing the relative placements.[30] Hydrogen evolution yields were improved with Co-polyoxometalate-TiO_2 in zeolite, but again, it is unclear how the sequence of charge separation occurs.[42] A directed nanoparticle arrangement in zeolite has only been recently realized using a novel two-photon photochemical reduction of Ag^+ in zeolite to generate Ag nanoparticles.[43] Very complex patterns were drawn in zeolite A single crystals with 250 nm resolution in the $x-y$ plane and 1 μm resolution in the z plane.

In summary, better synthetic strategies are required to place molecules and nanoparticles in zeolites in a directed fashion.

Many studies, as indicated above, show that in the dehydrated form, the zeolite framework can act as an electron donor or acceptor. In a few cases, there is spectroscopic evidence that the electron acceptor is a Na_4^{3+} species. However, in other cation-exchanged zeolites and even with some Na-zeolites, the acceptor species has not been definitely identified. The nature of the donor species is even murkier and is often proposed as the O atom of the Si—O—Al framework. A major difficulty in assessing the mechanisms of photoinduced electron transfer in zeolites is also the lack of quantum yield information of the initial charge-separated states; therefore, it is unclear how many of the encapsulated molecules are participating. With low charge separation efficiencies, other factors need to be taken into consideration. Zeolites often have trace redox-active metal impurities as part of the framework. There can also be different types of molecular defects, such as broken T—O—T bonds or T—OH groups which can participate in redox reactions. It has been shown that broken Ti—O—Ti bonds lead to lower coordinated titanium (penta or tetra), and Ti—OH groups in ETS-10 can oxidize the dye molecule 3′-(*p*-aminophenyl)-fluorescein.[44] If impurity/defect chemistry is involved in the electron−hole transfer reactions with photoexcited molecules, then the extent of reaction would be highly sample dependent. Hydration usually inhibits the framework-mediated charge-transfer reactions because it can minimize polarizing fields and can satisfy the coordinative unsaturation.

In summary, to better understand the role of the zeolite framework as electron/hole donor and for facilitating charge transport, the following are needed.

- Better quantitative information regarding the photoefficiency of the charge separation process needs to be established.
- The role of defect chemistry in the charge-transfer process needs to be determined. Quantitative measurement of

Research in the past three decades has clearly demonstrated that zeolites have a significant potential as an active host for novel light-driven chemistry, including providing important fundamental information on photochemistry in constrained charged spaces. Whether it will be a good host for practical solar-energy-driven processes depends on addressing some of the issues raised in this Perspective.

defects and/or intentional creation of defects and correlation with the photochemistry are essential.

For practical utilization of solar energy, zeolite-based systems provide several attractive features. As a host system, it can be manipulated under harsh chemical/environmental conditions. Zeolites exist over large length scales, from nanoparticles to macroscopic membranes. Zeolites can accommodate molecules, polymers, and solids. This diversity makes them a novel host for assembling complex superstructures. With improved synthetic skills of well-defined molecular assemblies in defined spatial geometry, improved charge separation yields are expected. This also holds true for nanoparticle assemblies. With controlled defect structures, the zeolite framework can play an active role in trapping photogenerated electrons and holes. Strategies for directional migration of charge along the framework, either due to zeolite framework composition (Ti—O—Ti nanowires) or by defect chemistry or via molecular species, are possible. Coupling the charge-separated species to catalysts, either homogeneous or heterogeneous, for chemical reactions can take advantage of the extensive body of work on zeolite-based catalysis. Large-scale assemblies can be built by aligning zeolite crystals or by using zeolite membranes. Research in the past three decades has clearly demonstrated that zeolites have a significant potential as an active host for novel light-driven chemistry, including providing important fundamental information on photochemistry in constrained charged spaces. Whether it will be a good host for practical solar-energy-driven processes depends on addressing some of the issues raised in this Perspective.

BIOGRAPHIES

Prabir K. Dutta received his Ph.D. degree in chemistry from Princeton University. After 4 years of industrial research at Exxon Research and Engineering Company, he joined The Ohio State University, where currently he is professor of chemistry. His research interests are in the area of microporous materials and ceramics, including their synthesis, structural analysis, hosts for chemical and photochemical reactions, application to sensors, and toxicity.

Michael Severance received his B.S. degree from The Ohio State University in 2008. He is currently working on his Ph.D. in analytical chemistry, focusing on the photophysical properties of donor—acceptor charge-transfer systems within zeolites.

REFERENCES

(1) Maeda, K.; Domen, K. Photocatalytic Water Splitting: Recent Progress and Future Challenges. *J. Phys. Chem. Lett.* **2010**, *1*, 2655–2661.

(2) Joshi, U. A.; Palasyuk, A.; Arney, D; Maggard, P. A. Semiconducting Oxides to Facilitate the Conversion of Solar Energy to Chemical Fuels. *J. Phys. Chem. Lett.* **2010**, *1*, 2719–2726.

(3) Ng, Y. H.; Iwase, A.; Kudo, A.; Amal, R. Reducing Graphene Oxide on a Visible-Light $BiVO_4$ Photocatalyst for an Enhanced Photoelectrochemical Water Splitting. *J. Phys. Chem. Lett.* **2010**, *1*, 2607–2612.

(4) Renger, T.; Schlodder, E. Primary Photophysical Processes in Photosystem II: Bridging the Gap between Crystal Structure and Optical Spectra. *ChemPhysChem* **2010**, *11*, 1141–1153.

(5) Wendell, D.; Todd, J.; Montemagno, C. Artificial Photosynthesis in Ranaspumin-2 Based Foam. *Nano Lett.* **2010**, *10*, 3231–3236.

(6) Shichi, T.; Takagi, K. Clay Minerals as Photochemical Reaction Fields. *J. Photochem. Photobiol., C* **2000**, 113–130.

(7) Wu, X.; Weare, W. W.; Frei, H. Binuclear TiOMn Charge-Transfer Chromophore in Mesoporous Silica. *Dalton Trans.* **2009**, 10114–10121.

(8) Calzaferri, G. Artificial Photosynthesis. *Top Catal.* **2010**, *53*, 130–140.

(9) Dutta, P. K.; Payra, P. Zeolites: A Primer. In *Handbook of Zeolites and Layered Materials*. Auerbach, S. M., Carrado, K. A., Dutta, P.K., Eds.; Marcel Dekker, Inc.: New York, 2003; pp 1—19.

(10) Treacy, M. M. J.; Higgins, J. B. *Collection of Simulated XRD Powder Patterns for Zeolites*; Elsevier: Amsterdam, The Netherlands, 2001.

(11) Simon, U.; Franke, M. E. Electrical Properties of Nanoscaled Host/Guest Compounds. *Microporous Mesoporous Mater.* **2000**, *41*, 1–36.

(12) Zhou, W. Microscopic Study of Crystal Defects Enriches our Knowledge of Materials Chemistry. *J. Mater. Chem.* **2008**, *18*, 5321–5325.

(13) Feldhoff, A.; Caro, J.; Jobic, H.; Ollivier, J.; Krause, C. B.; Galvosas, P.; Karger, J. Intracrystalline Transport Resistances in Nanoporous Zeolite X. *ChemPhysChem* **2009**, *10*, 2429–2433.

(14) Sokol, A. A.; Catlow, C. R. A. Local States in Microporous Silica and Aluminum Silicate Materials. 1. Modeling Structure, Formation, and Transformation of Common Hydrogen Containing Defects. *J. Phys. Chem. B* **2002**, *106*, 6163–6177.

(15) Belhadj, F.; Moissette, A.; Brémard, C. Long-Lived Electron—Hole Pair Formation through Photoionization of Diphenylacetylene Occluded in Medium Pores of Aluminum Rich M6.6ZSM-5 Zeolite ($M = Li^+, Na^+, K^+, Rb^+, Cs^+$) Influence of the Counterbalancing Cations on the Recombination Rate. *J. Photochem. Photobiol., A* **2009**, *208*, 203–212.

(16) Gener, I.; Moissette, A.; Bremard, C. Kinetics of Electron—Hole Pair Trapping via Photoionization of Biphenyl Occluded in Aluminium-Rich ZSM-5 Zeolites. Effects of Extra-Framework Cations. *Phys. Chem. Chem. Phys.* **2004**, *6*, 3732–3738.

(17) Moissette, A.; Marquis, S.; Cornu, D.; Vezin, H.; Bremard, C. Long-Lived Spin-Correlated Pairs Generated by Photolysis of Naphthalene Occluded in Non-Bronsted Acidic ZSM-5 Zeolites. *J. Am. Chem. Soc.* **2005**, *127*, 15417–15428.

(18) Moissette, A.; Bremard, C.; Hureau, M.; Vezin, H. Slow Interfacial Electron Hole Transfer of a *trans*-Stilbene Radical Cation Photoinduced in a Channel of Nonacidic Aluminum Rich ZSM-5 Zeolite. *J. Phys. Chem. C* **2007**, *111*, 2310–2317.

(19) Moissette, A.; Belhadj, F.; e Brémard, C.; Vezin, H. Kinetics and Characterization of Photoinduced Long-Lived Electron—Hole Pair of *p*-Terphenyl Occluded in ZSM-5 Zeolites. Effects of Aluminium Content and Extraframework Cation. *Phys. Chem. Chem. Phys.* **2009**, *11*, 11022–11032.

(20) Marquis, S.; Moissette, A; Bremard, C. Incorporation of Anthracene into Zeolites: Confinement Effect on the Recombination Rate of Photoinduced Radical Cation—Electron Pair. *ChemPhysChem* **2006**, *7*, 1525–1534.

(21) O'Neill, M. A.; Cozens, F. L.; Schepp, N. P. Photogeneration and Migration of Electrons and Holes in Zeolite NaY. *J. Phys. Chem. B* **2001**, *105*, 12746–12758.

(22) Keirstead, A. E.; Schepp, N. P.; Cozens, F. L. Influence of the Alkali Metal Cation on the Distance of Electron Migration in Zeolite Y: A Nanosecond Laser Photolysis Study. *J. Phys. Chem. C* **2007**, *111*, 14247–14252.

(23) Alvaro, M.; Atienzar, P.; Corma, A.; Ferrer, B.; Garcia, H.; Navarro, M. T. Photochemical Generation of Electrons and Holes in Germanium-Containing ITQ-17 Zeolite. *J. Phys. Chem. B* **2005**, *109*, 3696–3700.

(24) Ranjit, K. T.; Kevan, L. Photoreduction of Methyl Viologen in Zeolite X. *J. Phys. Chem. B* **2002**, *106*, 1104–1109.

(25) Hashimoto, S. Zeolites as Single Electron Donors for Photoinduced Electron Transfer Reactions of Guest Aromatic Species. Diffuse Reflectance Laser Photolysis Study. *J. Chem. Soc., Faraday T rans.* **1997**, *93*, 4401–4408.

(26) Coutant, M. A.; Sachleben, J. R.; Dutta, P. K. Effect of Rotational Mobility on Photoelectron Transfer: Comparison of Two Zeolite Topologies. *J. Phys. Chem. B* **2003**, *107*, 11000–11007.

(27) Sykora, M; Kincaid, J. R.; Dutta, P. K.; Castagnola, N. B. On the Nature and Extent of Intermolecular Interactions between Entrapped Complexes of $Ru(bpy)_3^{2+}$ in Zeolite Y. *J. Phys. Chem. B* **1999**, *103*, 309–320.

(28) Vitale, M.; Castagnola, N. B.; Ortins, N. J.; Brooke, J. A.; Vaidyalingam, A.; Dutta, P. K. Intrazeolitic Photochemical Charge Separation for $Ru(bpy)3^{2+}$—Bipyridinium System: Role of the Zeolite Structure. *J. Phys. Chem. B* **1999**, *103*, 2408–2416.

(29) Zhang, H.; Rajesh, C. S.; Dutta, P. K. Ruthenium Polypyridyl Complexes Containing a Conjugated Ligand L_{DQ} (L_{DQ} = 1-[4-(4′-methyl)-2,2′-bipyridyl]-2-[4-(4′-*N*,*N*′-tetramethylene-2,2′-bipyridinum)]ethene): Synthesis, Characterization, and Photoinduced Electron Transfer at Solution—Zeolite Interfaces. *J. Phys. Chem. C* **2009**, *113*, 4623–4633.

(30) Älvaro, M.; Chrétien, M. N; Fornés, V.; Galletero, M. S.; García, H.; Scaiano, J. C. Multicomponent Donor—Acceptor Relay System Assembled within the Cavities of Zeolite Y. Photoinduced Electron Transfer between $Ru(bpy)_3^{2+}$ and 2,4,6-Triphenylpyrylium in the Presence of Interposed TiO_2. *J. Phys. Chem. B* **2004**, *108*, 16621–16625.

(31) Borja, M; Dutta, P. K. Storage of Light Energy by Photoelectron Transfer Across as Sensitized Zeolite Solution Interface. *Nature* **1993**, *362*, 43.

(32) Kim, Y.; Das, A.; Zhang, H.; Dutta, P. K. Zeolite Membrane-Based Artificial Photosynthetic Assembly for Long-Lived Charge Separation. *J. Phys. Chem. B* **2005**, *109*, 6929–6932.

(33) Sykora, M.; Kincaid, J. R. Photochemical Energy Storage in Spatially Organized Zeolite-Based Photredox System. *Nature* **1997**, *387*, 162.

(34) Park, Y. S.; Lee, E. J.; Chun, Y. S.; Yoon, Y. D.; Yoon, K. B. Long-Lived Charge-Separation by Retarding Reverse Flow of Charge-Balancing Cation and Zeolite-Encapsulated $Ru(bpy)_3^{2+}$ as Photosensitized Electron Pump from Zeolite Framework to Externally Placed Viologen. *J. Am. Chem. Soc.* **2002**, *124*, 7123–7135.

(35) Kim, Y. I.; Keller, S. W.; Krueger, J. S.; Yonemoto, E. H.; Saupe, G. B.; Mallouk, T. E. Photochemical Charge Transfer and Hydrogen Evolution Mediated by Oxide Semiconductor Particles in Zeolite-Based Molecular Assemblies. *J. Phys. Chem. B* **1997**, *101*, 2491–2500.

(36) Kim, Y; Dutta, P. K. An Integrated Zeolite Membrane/RuO_2 Photocatalyst System for Hydrogen Production from Water. *J. Phys. Chem. C* **2007**, *111*, 10575–10581.

(37) Yoon, K. B.; Park, Y. S.; Kochi, J. K. Interfacial Electron Transfer to the Zeolite-Encapsulated Methylviologen Acceptor from Various Carbonylmanganate Donors. Shape Selectivity of Cations in Mediating Electron Conduction through the Zeolite Framework. *J. Am. Chem. Soc.* **1996**, *118*, 12710–12718.

(38) Ryu, S. Y.; Balcerski, W.; Lee, T. K.; Hoffmann, M. R. Photocatalytic Production of Hydrogen from Water with Visible Light Using Hybrid Catalysts of CdS Attached to Microporous and Mesoporous Silicas. *J. Phys. Chem. C* **2007**, *111*, 18195–18203.

(39) Jeong, N. C; Kim, H. S.; Yoon, K. B. New Insights into CdS Quantum Dots in Zeolite-Y. *J. Phys. Chem. C* **2007**, *111*, 10298–10312.

(40) Wong, K-L; Souici, A.; Waele, V. D.; Mostafavi, M.; Metzger, T. H.; Mintova, S. Subnanometer CdS Clusters Self-Confined in MFI-Type Zeolite Nanoparticles and Thin Films. *Langmuir* **2010**, *26* (6), 4459–4464.

(41) Guan, G.; Kida, T.; Kusakabe, K.; Kimura, K.; Fang, X.; Ma, T.; Abe, E.; Yoshida, A. Photocatalytic H_2 Evolution under Visible Light Irradiation on CdS/ETS-4 Composite. *Chem. Phys. Lett.* **2004**, *385*, 319–322.

(42) Dubey, N; Rayalu, S. S.; Labhsetwar, N. K.; Devotta, S. Visible Light Active Zeolite-Based Photocatalysts for Hydrogen Evolution from Water. *Int. J. Hydrogen Energy* **2008**, *33*, 5958–5966.

(43) De Cremer, G.; Sels, B. F.; Hotta, J.-i.; Roeffaers, M. B. J.; Bartholomeeusen, E.; Coutino-Gonzalez, E.; Valtchev, V.; De Vos, D. E; Vosch, T.; Hofkens, J. Optical Encoding of Silver Zeolite Microcarriers. *Adv. Mater.* **2010**, *22*, 957–960.

(44) Tachikawa, T.; Yamashita, S.; Majima, T. Probing Photocatalytic Active Sites on a Single Titanosilicate Zeolite with a Redox-Responsive Fluorescent Dye. *Angew. Chem., Int. Ed.* **2010**, *49*, 432–435.